Absorption, Luminescence, Resonance Raman, and Resonance CARS Spectroscopy on FBS Diacetylene Single Crystals with Color Zones

A. Materny and W. Kiefer*

Institut für Physikalische Chemie der Universität Würzburg, Marcusstrasse 9-11, W-8700 Würzburg, Federal Republic of Germany

Received December 11, 1991

ABSTRACT: We have made investigations on color zones in FBS diacetylene single crystals by means of various optical spectroscopical methods in order to derive a plausible model for the origin of this type of chromism. Absorption, luminescence, resonance Raman, and CARS spectroscopy revealed that most probably growth defects in {111} crystal growth sectors influence the side group geometry of FBS polymer chains. This results in shortening of the π-electron conjugation lengths and in consequence in an anti-Stokes shift of electronic and vibrational transition frequencies. Particularly, resonance CARS spectroscopy proves to be a new valuable tool for the investigation of electronic and structural properties of the FBS crystals.

Introduction

There is a growing interest in polydiacetylenes (PDAs) from a basic as well as an applicational point of view. The linear and nonlinear optical properties associated with the conjugated backbone of PDAs have attracted the attention of many researchers over the past 20 years. Due to the great variety of substitutional side groups, a large number of different PDAs could be synthesized, since the discovery by Wegner.[1] Particular properties of these polymers are the reversible and irreversible color changes of various kinds, known as thermochromism,[2–5] solvatochromism,[6,7] photochromism,[8] and other forms as for example pressure-induced chromism.[9] These chromisms lead to changes in the absorption and also in the Raman spectra. A number of extensive studies have been carried out; however, the molecular mechanism giving rise to the chromic transition is still a controversial subject. The key to this problem seems to be connected to the understanding of the sensitivity of the electronic properties to polymer backbone conformation.

Figure 1 shows the topochemical solid-state polymerization, which the diacetylene monomers (DAs) undergo upon thermal annealing or exposure to high-energy radiation. From this reaction polymer chains are formed, which have a substantial π-electron delocalization, forming a pseudo-one-dimensional electronic system. The extended, conjugated, π-bond structure can be described by two resonance forms, the acetylene (Figure 1a) and the butatriene (Figure 1b) structure. Suppositions that a change between the two mesomeric structures causes the observed color changes[10] are casted doubt on by recent experimental and theoretical results.[11] The assumption that interruptions of the conjugation length are the true reason for color effects arose relatively early[12] and is the most accepted one by now. Such interruptions could be caused by configurational or chemical defects. Transitions from a planar to a nonplanar form of the PDA chain do explain shifts to higher energies in the absorption spectrum. The planar–nonplanar conformational change in the backbone results in a shorter conjugation length. In this connection, an essential influence of the side groups has been proved by experiments[3] as well as by theoretical considerations.[11]

A special form of chromism was introduced very recently.[13] In the reddish monomer crystals of the DAs TS6, FBS, and TS/FBS (Table I) sharply separated yellow zones were observed. These color zones show a blue-shifted absorption (Y-absorption) in addition to the normally seen red absorption. The red absorption (P-absorption) results from polymer chains, which originate during crystal growth. The TS6, FBS, and TS/FBS crystals are single crystals, in which all polymer chains lie parallel to the b-axes of the crystal. A typical appearance of color zones is presented in Figure 2, together with the axes of the monoclinic crystal lattice.

The color zones in these DAs have been already characterized by absorption and luminescence spectroscopy.[13] The aim of the present work is a more accurate investigation of the observed chromism by making use of several optical spectroscopic methods. We believe that by these methods more evidence of the electronic and structural nature can be gained. Here, we present experimental results from absorption, luminescence, resonance Raman, and resonance CARS (coherent anti-Stokes Raman scattering) measurements and we compare our results to those obtained for other types of chromism. A theoretical interpretation by means of Franck–Condon calculations is presented elsewhere.[14–16]

We demonstrate our experimental results on examples for FBS DA crystals. Results for TS/FBS and TS6 will be published in a subsequent paper.[16] In our work we considered crystals with low polymer content, where the polymer chains are embedded in the monomer matrix. A color effect in these crystals therefore should be seen as a single-chain phenomenon[17] rather than a result of aggregation.[18]

Experimental Section

The symmetrically substituted FBS DA is prepared by the method described by Wegner.[1] The lozenge-shaped monoclinic crystals were obtained from solution and had less than 1% contents of polymer. The freshly grown DA crystals were cleaved parallel to the 100 surface (containing *b*- and *c*-axes, Figure 2) to produce thin platelets of about 50-μm thickness and about 3-mm length in the chain direction (∥ *b*-axis). To obtain spectra with higher signal to noise ratios and because of the enormous heat sensitivity of the DA single crystals, we cooled them down to a temperature of about 10 K. Because of the high optical anisotropy of the DA crystals, caused by the parallel polymer chains, the polarization of light in all experiments was choosen to be parallel to the *b* axis.

The experimental setup used for absorption and fluorescence spectroscopy has been described elsewhere.[13] For the resonance

---

* To whom correspondence should be addressed.

0024-9297/92/2225-5074$03.00/0

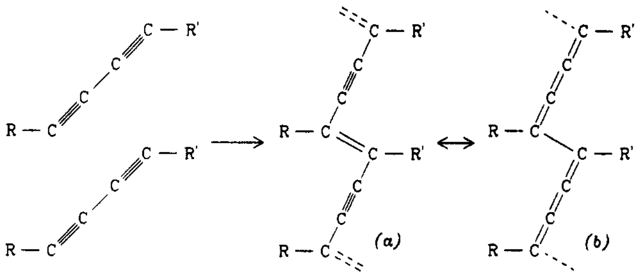

Figure 1. Topochemical solid-state polymerization of diacetylene monomers with mesomeric backbone structures of the polymer: (a) acetylene and (b) butatriene form.

Table I
Substituents of FBS, TS6, and TS/FBS Diacetylenes

diacetylene	substituent
FBS	R = R': –CH_2–O–SO_2–Ph–F
TS6	R = R': –CH_2–O–SO_2–Ph–CH_3
TS/FBS	R ≡ TS6, R' ≡ FBS

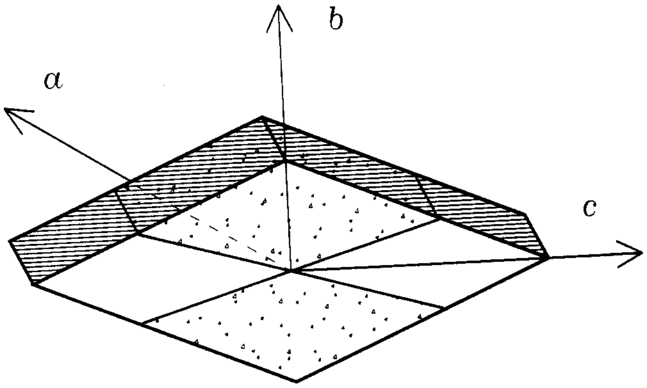

Figure 2. Schematic form of FBS, TS/FBS, or TS6 single crystals. Arrows indicate crystal axes of the monoclinic lattice. The speckled areas show a typical shape of the yellow color zones (Y-zone).

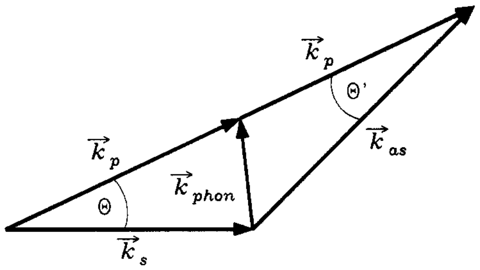

Figure 3. Momentum (wave) vectors for the CARS process. $\vec{k}_p$, $\vec{k}_s$, and $\vec{k}_{as}$ are the momentum vectors of the pump, Stokes, and CARS beam, respectively. $\vec{k}_{phonon}$ is the momentum vector for the phonon. θ is the crossing (phase) and θ' the collection angle.

Raman spectroscopy a micro Raman setup with an OMA detector was used.[19] A back-scattering arrangement was chosen, where the incident laser light hit the crystal perpendicular to the 100 plane. The setup for the pulsed solid-state CARS measurements has also been described elsewhere in detail.[20] Applying two dye lasers, we were able to perform resonance CARS spectroscopy. The pump laser beam was aligned vertically to the 100-surface of the crystal. In order to excite particular phonons in the single crystals, the difference between the pump and Stokes beam wave vector must coincide with the wave vector of the coherently excited phonons in the crystal, i.e. $\vec{k}_p - \vec{k}_s = \vec{k}_{phonon}$ (Figure 3). This phase-matching condition was achieved by changing the crossing angle θ between the pump and Stokes beam as well as the orientation of the plane spanned by the pump and Stokes beam, relatively to the crystal *b*-axis.

The Raman as well as the CARS setup allowed us to obtain additional absorption spectra before each measurement. In all experiments a strict separation between the P- and Y-zones of the crystals was obtained by cleaving the crystals or by appropriate covering of the P- or Y-zone. Some more experimental details are given in the next section together with experimental results.

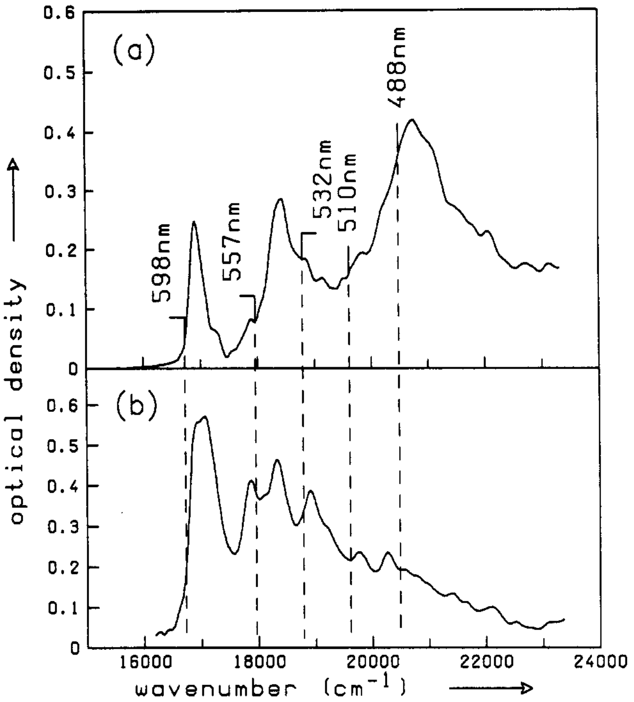

Figure 4. Absorption spectra of an FBS DA crystal with color zones recorded at a sample temperature of 10 K. The polarization of the transmitted light is parallel to the crystal *b*-axis. (a) shows the absorption spectrum of the Y-zone, and (b) that of the P-zone. Vertical lines with numbers indicate the wavelength positions of the pump laser, employed for excitation of the CARS spectra shown in Figure 9.

Results and Discussion

FBS Y-zones do have a yellow or orange color. This variation of color is likely caused by changes of the electronic properties of the Y-zone. From TS/FBS we know, that the Y-absorption shows a similar vibronic structure as compared to the absorption spectrum of the polymer chains.[13] Consequently, it is reasonable to assume that polymer chains cause the Y-absorption, which is in agreement to the statements made in the Introduction. Figures 4a and 4b show a typical absorption spectrum for the Y- and the P-zone of an FBS DA crystal, respectively. The P-zone absorption (Figure 4b) shows the 0–0 transition at about 17 000 cm^{-1} with fairly well-resolved vibronic structure. From the position of the absorption peak one can conclude that the polymer chains do have a length of less than about 20 monomer units.[21] In the Y-zone (Figure 4a) the absorption spectrum differs substantially from the one reproduced in Figure 4b. The 0–0 line belonging to the P-absorption is slightly shifted to higher frequencies, which could mean that the P-chains are a little bit longer in the Y-zone than in the P-zone. There are at least two broad bands belonging to the additional Y-absorption, with presumable 0–0 transitions at about 18 500 and 20 800 cm^{-1}. The variation of the color of Y-zones seen in different DA crystals can of course also be observed in the absorption spectra. Figure 5 shows the Y-zone absorption spectrum of another FBS DA crystal with a distinct different absorption spectrum. There, also bands different from the P-zone absorption in Figure 4b can be recognized. In both cases (Figures 4a and 5) the vibronic structure of these bands is difficult to see and therefore absorption spectroscopy alone even performed at low temperatures does not give sufficient information.

A good way to derive additional information about electronic as well as structural properties is resonance Ra-

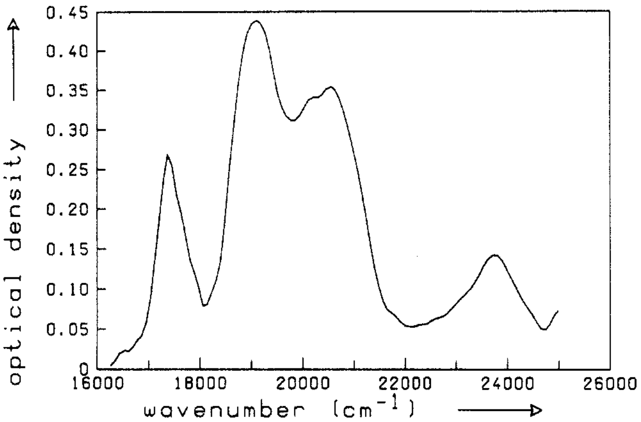

Figure 5. Absorption spectrum of a Y-zone of an FBS DA crystal at 10 K. Polarization of light is parallel to the crystal *b*-axis. For comparison see Figure 4a.

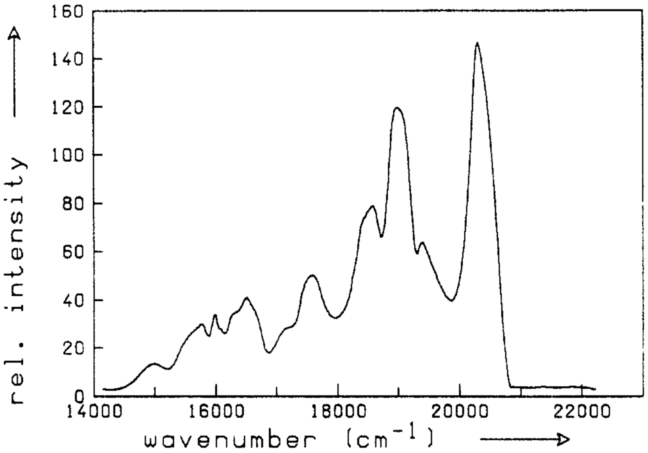

Figure 6. Typical luminescence spectrum of a Y-zone of an FBS DA crystal at about 10 K. The excitation wavelength was 325 nm. Polarization of incident and emitted light is parallel to the crystal *b*-axis.

man spectroscopy. Many investigations where made on PDAs by Raman spectroscopical methods concerning chromatic properties.[12,22-25] In none of them have problems been reported when Raman spectra are taken from different color forms of the PDAs. We noticed that in FBS crystals luminescence can be observed when the Y-zone is irradiated by light with higher energy than of the Y-absorption. This luminescence is structured and is extremely strong. A typical luminescence spectrum arising from the Y-zone of an FBS DA crystal is shown in Figure 6. Because of this luminescence, resonance Raman spectroscopy with excitations interesting for an investigation of the color zones is not possible.

There are several possibilities to obtain information on Y-zones from resonance Raman spectra. One is for instance to investigate Y-zones of crystals with very weak color zones by varying the excitation frequency and resonantly enhancing the different electronic transitions. One other is to excite Raman spectra of crystals with very strong color zones by choosing an out of resonance, i.e. a low frequency excitation, and comparing the spectra of the P- and Y-zones. Neither of them is really satisfactory. Figure 7 for example shows resonance Raman spectra of an FBS DA crystal with a very significant Y-zone excited with about 5 mW of 632.8-nm laser line. PDA chains, if resonantly enhanced, exhibit only a few Raman lines, which all belong to symmetric A_g modes of the PDA backbone.[26] In the wavenumber region from 3500 to 500 cm^{-1} only four prominent Raman lines, labeled ω_1 to ω_4, and about six combination frequencies can be seen if resonance conditions are fulfilled.[27] Parts a and b of Figure 7 exhibit parts of the resonance Raman spectrum of the P-zone of an FBS DA crystal. In Figure 7a the ω_1 line (C≡C stretching) at about 2040 cm^{-1} belonging to the polymer chains in the P-zone (from here on called ω_{1P}) is shown. In Figure 7b a doublet can be seen at about 1470 and 1455 cm^{-1}. These Raman lines can be assigned to the ω_2 mode (C=C stretching, from here called ω_{2P} for the P-chains) and to a Fermi resonance enhanced CH_2-scissors vibration (ω_{CH_2}) belonging to the side group,[28] respectively. Parts c and d of Figure 7 show the same spectral regions for the Y-zone. The ω_{1P} and $\omega_{2P}/\omega_{CH_2}$ modes belonging to the P-chains are slightly shifted to higher frequencies. The $\omega_{2P}/\omega_{CH_2}$ doublet is partly hidden under a new line belonging to Y-chains. This ω_{2Y} line has its frequency at about 1480 cm^{-1}, whereas the ω_{1Y} line is at about 2090 cm^{-1}. We are not able to correlate the Y-resonance Raman lines to any feature in the Y-absorption spectrum.

The DA crystals are extremely sensitive against heating, which leads to a further polymerization and/or to a destruction of the DA crystal. Therefore laser irradiation with frequencies in resonance with the strong absorption of the polymer chains changes spectral conditions or even destroys the crystal. Even cooling down the crystal to about 10 K does not prevent destruction of the crystal if moderate laser power is employed. With the application of only very little laser power, constant conditions in the crystals could be achieved when the sample is irradiated. Anti-Stokes Raman spectra would be free of luminescence. However, since the crystal has to be cooled down to about 10 K, there is no more observable Raman intensity for the modes to be detected.

On the other side, CARS spectroscopy seems to be a favorable method for obtaining information of both electronic and structural properties. Recent CARS investigations[20] showed that it is possible to obtain coherent anti-Stokes Raman signals with fairly good signal to noise ratio. For a detailed description of the CARS process we refer to refs 29 and 30. In Figure 8 we display schematically the CARS process. Varying the pump laser frequency ω_p enables one to investigate the resonance behavior of the CARS lines. From the CARS experiments on P-form DA crystals we expect an extreme enhancement of the signal when in resonance with the ^1A_g–^1B_u transitions of the delocalized π-electron system of the polymer backbone. The nonlinear optical properties of PDAs showing chromisms have already been investigated.[4] It was shown by third harmonic generation measurements that also the Y-form of the investigated PDA films exhibits remarkable values for the third-order nonlinear susceptibility ($|\chi^{(3)}|$) which are only a little smaller than those measured in P-form films.

Figure 9 shows CARS spectra obtained from an FBS DA crystal in the P-zone (Figure 9a,b) and the Y-zone (Figure 9c–l). The spectra were taken for different pump laser wavelengths λ_p, as labeled in the figures. The spectra displayed are all corrected for different laser intensities, detection sensitivity, and linearity, and also for absorption. The scales for the CARS intensities are therefore comparable to each other. For comparison we refer to Figure 4 where the absorption of both the Y-zone and the P-zone of that crystal is shown, from which the CARS spectra were taken. As mentioned above, the pump wavelengths λ_p are marked in the absorption spectra.

Before discussing the CARS spectra, we emphasize two crucial points which have to be considered when CARS spectra are taken from these crystals. As mentioned above, the crystals are very sensitive to laser light, which forces one to use only very little laser power. Especially in the Y-zone we observed changes in the CARS spectra if too high laser power has been employed. The spectra obtained

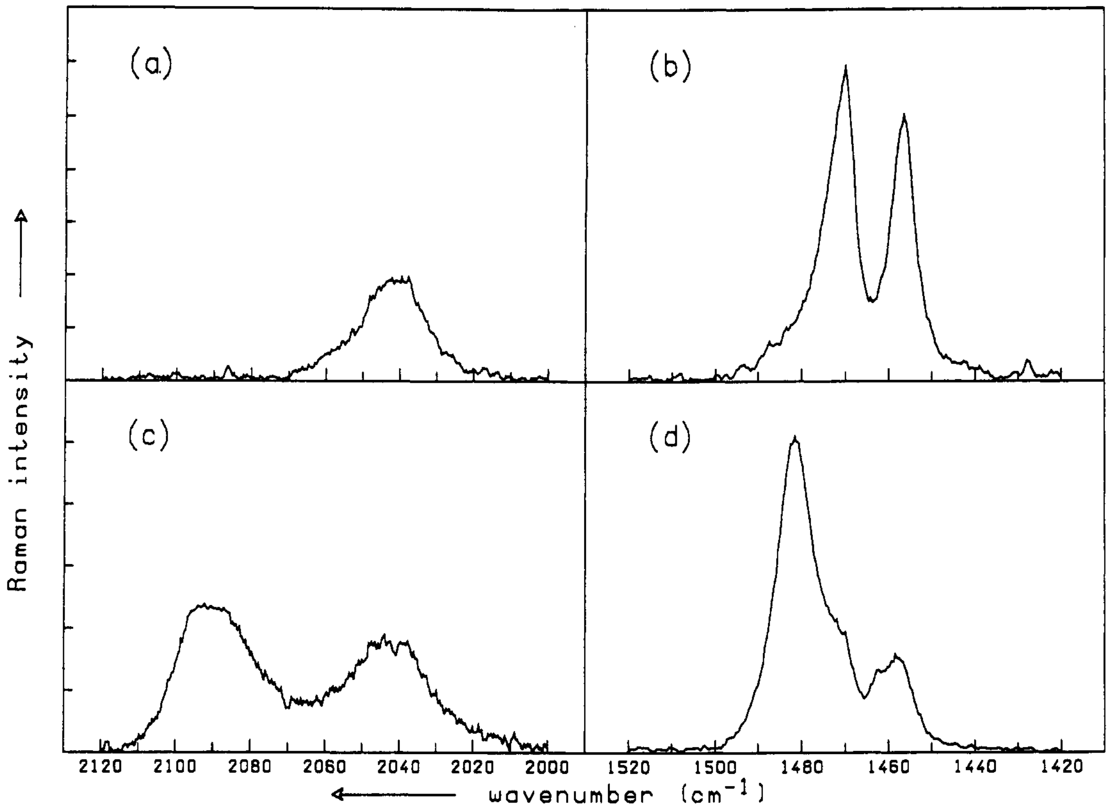

Figure 7. Raman spectrum of an FBS DA crystal at 10 K, for excitation wavelength $\lambda_0 = 633$ nm. Polarization of incident and scattered light is parallel to the *b*-axis of the crystal. Spectra on the left side (a and c) correspond to the C≡C stretching, and those on the right side (b and d) to the C=C stretching region of the P- and Y-zones. For further information, see text.

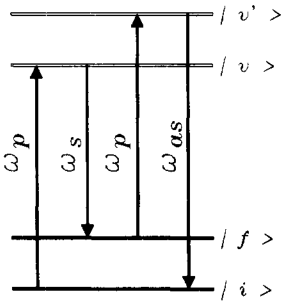

Figure 8. Schematical representation of the CARS process. $|i\rangle$ and $|f\rangle$ are the initial and final state of the Raman process, respectively. $|v\rangle$ and $|v'\rangle$ are intermediate states of the CARS process. ω_p, ω_s, and ω_{as} are the frequencies of the pump, Stokes, and CARS beam, respectively.

at very low laser energy (order of 1–10 μJ) have been repeated several times. Even under these conditions we sometimes have been unsuccessful in recording CARS spectra when excited at exact resonance within the electronic 0–0 transition. The noise inherent in the unsmoothed CARS spectra therefore originates from the low laser power employed.

The second point worth mentioning is that both the intensity and frequency of the CARS lines (same is valid for Raman spectroscopy) could shift considerably when the spot position on the crystal surface is changed. This arises from inhomogeneities in the monomer crystals and reveals a distribution of relative short chains in their monomer matrices. As shown earlier,[13,31] short chains (up to about 30 monomer units) do have discernible optical properties. Comparisons are therefore only meaningful if complete spectra are taken from one crystal spot in the actual color zone, containing the ω_{1P}, $\omega_{2P}/\omega_{CH_2}$ and the ω_{1Y}, ω_{2Y} modes. Changing of dyes is therefore not possible while the spectrum is taken, which otherwise would have required a realignment of the laser beams. Only if ω_p had to be changed were different dyes used. In this case we tried to hit always the same spot in the crystal. There are only a few combinations of dyes for pump and Stokes lasers which allow CARS spectra to be taken over a complete range of about 900 cm^{-1}. As a consequence we could only choose a specific set of values for ω_p.

The phase-matching conditions were kept as follows. The phonon momentum vector $\vec{k}_{\text{phonon}}$ was set parallel to the *b*-axis, which means parallel to the extent of the conjugated π-electron system of the polymer backbones. For other cases no remarkable CARS signal could be detected. The applied phase angle θ (Figure 3) was relatively small (1–3°) and had no measurable dispersion. In addition, there was no difference in θ for the P- and Y-zones. This fact can be easily explained. The DA crystals represent a system which can be compared with a solution at low concentration, where the polymer chains are randomly distributed in the monomer matrix. Therefore, the phase angle is determined by the monomers rather than by the polymers, as long as the concentration is not too high. The monomer matrices do not absorb in the visible region and therefore the refractive index does not show remarkable dispersion in this region. This results in only a small, nearly constant phase angle. The polarization of the ω_p, ω_s, and ω_{as} beams was chosen to be parallel to the chains.

The CARS-spectra in Figure 9, together with the absorption spectra in Figure 4 allow an insight in the nature of the Y-zone. The spectra of the P-zone only exhibit the ω_{1P} and $\omega_{2P}/\omega_{CH_2}$ lines for all pump laser wavelengths λ_p. In Figure 9a,b such a CARS spectrum is shown as an example for 598-nm excitation. The same lines can be observed in the Y-zone when exciting by the same wavelength (Figures 9c,d), which means excitation near the P-(^1A_g–^1B_u) transition. For this case nearly no additional features in the spectrum are found. In Figure 9c a slight indication for a new line can be seen at higher wavenumbers. At about this position a new band occurs for 557-nm excitation (s. Figure 9e). This band seems to

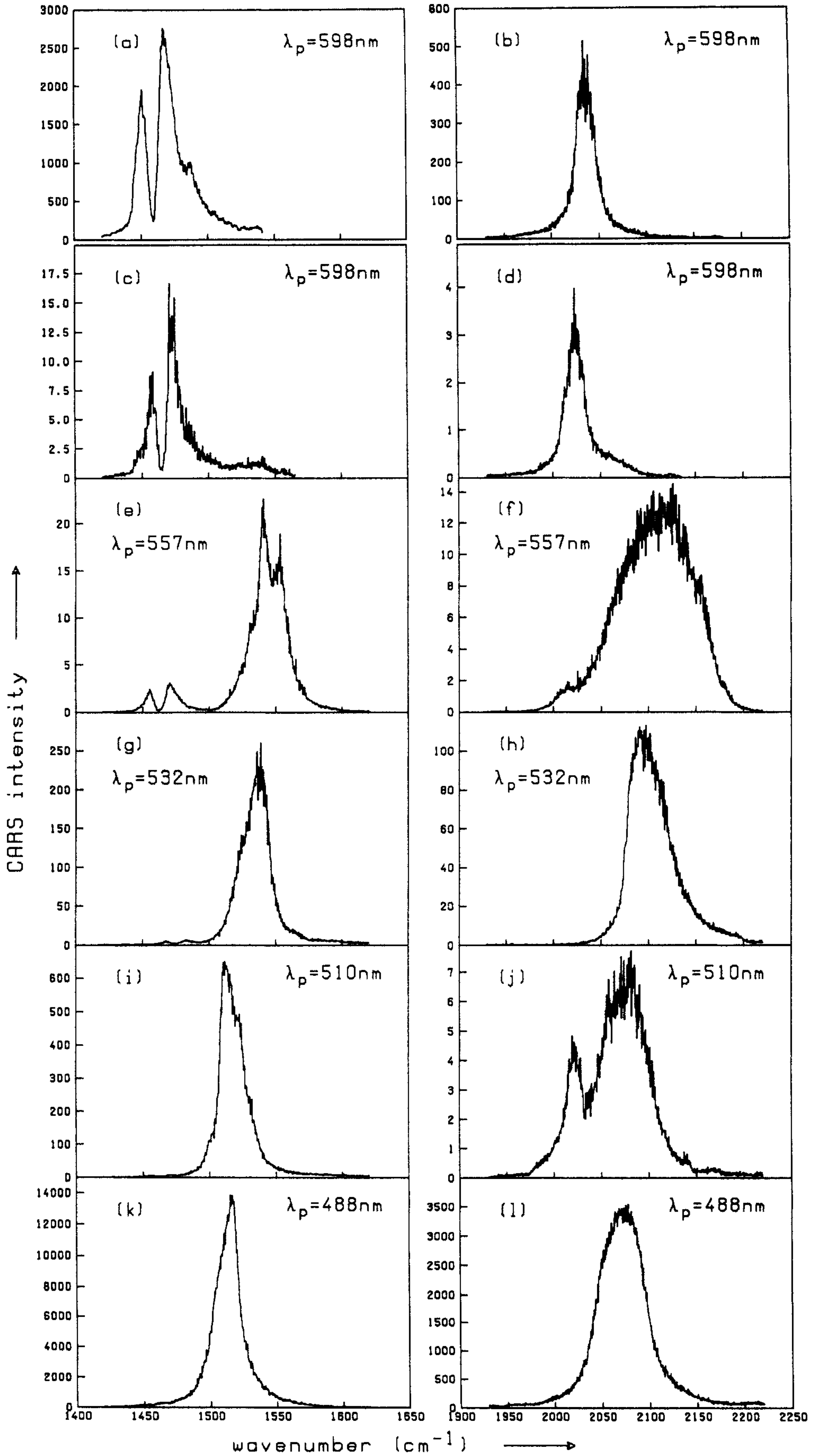

Figure 9. Resonance CARS spectra of an FBS DA crystal at 10 K. The pump wavelength λ_p used is labeled for each spectrum. For comparison with the absorption spectra of this crystal, see Figure 4. (a) and (b) show CARS spectra of the P-zone, and (c)–(l) those for the Y-zone. Spectra on the left side correspond to the C=C stretching region, and those on the right side to the C≡C stretching region. For further details, see text.

have contributions from at least two lines. Figure 9f shows a striking broad band for the ω_{1Y} mode which supports this assumption. ω_{1P} is only seen as a shoulder of the Stokes side of the ω_{1Y} band, while $\omega_{2P}/\omega_{CH_2}$ is well to be recognized in Figure 9e. The pump laser wavelength at 557 nm is located on the Stokes wing of a band, which shows up strongly in the absorption spectrum of the Y-zone at about 18 400 cm^{-1} (Figure 4a). Note that the band at about 18300 cm^{-1} in the absorption spectrum of the P-zone is due to a vibronic band. The next λ_p we have chosen at 532 nm is at the anti-Stokes side of this feature. In Figure 9g,h we display the CARS lines for the C=C and C≡C stretching regions, respectively. Both lines (ω_{1Y} and ω_{2Y}) are positioned in the lower energy region of the two broad bands displayed in Figure 9e,f. This indicates that two lines are hidden under the bands shown in Figure 9e,f, bands which are assigned to polymer chains with two different ^1A_g–^1B_u transitions. With 532-nm excitation mainly the higher energy transition is in resonance which results in an enhancement of the associated ω_{1Y} and ω_{2Y} line. To investigate the next strong band at about 20 700 cm^{-1} in the Y-absorption spectrum, we chose wavelengths at 510 and 488 nm for the pump laser beam. For both excitations new ω_{1Y} and ω_{2Y} lines show up at the same spectral position (Figure 9i–l). These bands are shifted to lower frequencies as compared to the bands observed for 532 nm. The spectrum in Figure 9j exhibits in addition a line at the ω_{1P} position. Franck–Condon calculations show that for 510-nm excitation the excitation profile for the ω_{1P} Raman and CARS mode has a maximum.[16] Therefore, the occurrence of the ω_{1P} line in Figure 9j seems to be comprehensible. For λ_p at 488 nm we placed the excitation wavelength near the maximum of the strongest feature of the Y-absorption spectrum. Because of very high absorption for this wavelength we succeeded in taking CARS spectra without destroying the crystal at the spot where the focus of the pump and Stokes laser hit the crystal surface only after several attempts. The observed ω_{2Y} and ω_{1Y} lines (Figure 9k,l) are very strong and do have about the same width and position as the CARS lines observed for 510-nm excitation. No enhancement of any other CARS lines can be seen when the pump laser wavelength is varied from 510 to 488 nm. This indicates that no more ^1A_g–^1B_u 0–0 transitions are between the two strong absorption bands belonging to the Y-zone. The experimental limit for λ_p was at about 460 nm. However, in the region 488 nm < λ_p < 460 nm we were unable to obtain reliable CARS spectra, because of a fast decrease of line intensity, originating most probably from destruction of the sample. The observed line positions remained at about the same frequency region as those observed for 488-nm excitation.

We believe that our measurements strongly support the model which explains chromism effects by a change in the conjugation length of the polymer backbone's π-electron system. By application of resonance Raman and resonance CARS spectroscopy, selective enhancement of vibrations is possible for those domains in which electronic transitions coincide with the exciting wavelength. The FBS crystal studied during our investigations revealed besides the P-domain at least three new domains in the Y-zone. It remains the question whether shorter chain lengths or interruptions of longer chains are responsible for the occurrence of chromism in FBS crystals. Both effects would explain a blue shift in absorption, as has been shown by Exarhos et al.[12] by applying a simple free electron gas model to PDAs. There are two points which support the assumption that interruption of conjugation is the reason for the observed features seen in the FBS Y-zone. First, there is no conformity between the observed features seen in FBS Y-absorption spectra with measured absorption of DA oligomers of FBS.[21] Second, if there would be separate chains of short length one would expect a blue shift in absorption for decreasing chain length combined with an increase of Raman frequency for the C=C and C≡C stretching mode. Such observations have been made for *tert*-butyl-capped polyenes[32] and for polyacetylenes.[33] However, our results are contrary to these observations. The measured positions for the CARS lines shift to lower energies when excitation is coming into resonance with the electronic transition of higher energy.

Investigations on PDA and DA crystals containing defects showed that luminescence occurred near defects, if irradiated by blue light,[13,34] which are not as structured but similar to that in Figure 6. Fluorescence spectroscopy of stable FBS DA oligomers also exhibits structured spectra similar to that of Figure 6, while defect-free PDA crystals, containing long polymer chains do not show remarkable luminescence.[35] Defects as the proper cause of chromism in the three mentioned DAs, FBS, TS6, and TS/FBS, may be confirmed by the following experimental results. The observation of sharp color zones in DA crystals was first described for TS/FBS crystals.[13] TS6 crystals showed sometimes color zones whereas in FBS crystals these color zones were more frequently observed. The appearance of color zones seems to depend on the growth condition of the crystals. On the {100} surface of the crystals zones of different roughness could be observed. These surface zones in most cases correspond to the P- and Y-zones of the crystals. This observation makes it most probable that crystal defects interrupt the conjugation of the π-electron system, which leads to shorter conjugation lengths and in consequence to higher absorption frequencies. Recently, Eckardt et al. suggested that the high energy-shift in absorption as well as in the stretching frequency originating from a P- to Y-form change in PDAs can be understood as an effect of strain, induced by substituents.[11] These authors used VEH and MNDO calculations to explain the influence of side group angle relative to the PDA backbone on optical properties of PDAs. They found that side group distortions needed to produce spectral shifts, seen for chromatic transitions, lead only to subtle rearrangements of backbone geometry. Crystal defects, which are only a small hindrance for the side groups therefore could effect the formation of Y-zones. The different frequencies of the appearance of color zones in DAs containing different substituents (Table I) strongly point to a main role of side group geometry as a cause for chromism in these DA crystals.

There are still two essential questions opened: (i) why do the observed CARS frequencies of the Y-chains shift to lower frequencies for shorter conjugation lengths? As discussed above one expects an opposite effect. A possible explanation for this is that the defects locally influence the Y-chains. These defects try to turn the side groups, which results in a blue shift for the absorption as well as for the Raman frequencies. If only one substituent is turned in respect to the others, the strain should be greater than if more substituents are turned in the same direction. Therefore, a separation into shorter parts results in a more relaxed chain with a Stokes shift for the vibrational frequencies. However, we have to mention that no experimental proof can be given for this explanation when the methods discussed above are applied. A calculation similar to the one reported by Eckhardt et al.[11] would definitely give more insight into this problem. (ii) The second question is why there exist sharply separated color zones rather than a homogeneous distribution of Y-chains over the whole crystal. Different investigations (see ref 13 and references therein) showed that edge dislocations are preferrably situated in {111} growth sectors. A strain field upon monomer molecules is forced by small-angle grain boundaries formed by dislocations having a Burgers vector in the *b*-direction ([010]). Taking into account the arguments given above, the origin of color zones in DA crystals may be explained by supposing that the {111} growth sectors coincide with the observed color zones.

Conclusion

In general, DA polymer chains show color effects. The simultaneous occurrence of two well-separated color forms in FBS, TS/FBS, and TS6 DA crystals motivated us to investigate the origin of these color zones in detail by applying various spectroscopic techniques. In order to elucidate these chromism effects in PDAs we particularly studied the color zones of FBS DA crystals by absorption, luminescence, resonance Raman, and resonance CARS spectroscopy. From absorption spectra of FBS a first interpretation of the color effects was obtained. One result was that the absorption of the Y-zone contains different features, which can be ascribed to different polymer chains in the DA crystals. From the observed high-frequency position of these features, seen in addition to the P-absorption lines, and from the observation of well-structured luminescence in the Y-zone, we conclude that the Y-zones contain shorter conjugation lengths than the P-chains. Applying resonance Raman spectroscopy, we tried to gain more structural information from the Y-chains. These results were combined with those obtained from absorption spectroscopy. However, there are limitations of this type of spectroscopy because of the strong luminescence arising from the Y-zones. Nevertheless we could observe that Y-chains exhibit vibrational frequencies which are shifted to higher frequencies than those observed for P-chains. We found that resonance CARS spectroscopy is an excellent method for this type of investigation. This is due to the fact that by this coherent method there are no problems with luminescence and simultaneously the same spectral information can be obtained, as is possible by linear resonance Raman spectroscopy.

Besides some problems caused by the sensitivity of the DA crystals, we gained sufficient information by this nonlinear method to characterize the nature of Y-chains far more precisely. Considering various results and calculations published elsewhere and taking into account our own observations of defect structures visible on the DA crystal surfaces, we were able to present a plausible model for the origin of color zones. In this model, {111} growth sectors containing edge dislocations act as defects on side groups of DA crystals and therefore shift the electronic as well as the vibronic energies. The latter is due to the change of the conjugation length of the π-electrons in the polymer backbones. In our opinion the disturbance of the planarity of the polymer backbone is the cause for nearly all chromism effects in DA polymers. Although there are several reasons for such a disturbance, we believe that it is mainly caused by side group geometry effects. This also explains the strong dependence of chromisms from the chemical groups substituted to the DAs.

In addition we have shown that resonance CARS spectroscopy is an excellent tool to examine electronic and structural properties of systems which are not accessible by linear resonance Raman spectroscopy. Until now only very little work has been done by applying CARS spectroscopy in solids, and even less at resonance conditions. Probably two reasons did prevent such measurements in the past: (i) many substances were destroyed because of application of relatively high laser powers; (ii) in most cases it is not possible to obtain layers thin enough that the laser beams as well as the generated CARS beam can penetrate the highly absorbing solid material. Different approaches would be by the study of the absorbing materials solved in nonabsorbing matrices or by a backscattering CARS arrangement as proposed by Pfeiffer et al.[36] The latter method would open many new applications to resonance CARS spectroscopy.

Acknowledgment. We wish to thank Professor Markus Schwoerer, University of Bayreuth, for making the DA crystals available to us. Some of the absorption measurements were performed in his laboratory. We are very grateful to Mrs. Irene Müller for growing the excellent crystals. A.M. thanks the Stiftung Volkswagenwerk and the Fonds der Chemischen Industrie for a postgraduate scholarship. Financial support from the Verband der Chemischen Industrie e.V. and the Deutsche Forschungsgemeinschaft is highly acknowledged.

References and Notes

(1) Wegner, G. Z. *Naturforsch., B: Anorg. Chem., Org. Chem., Biochem., Biophys. Biol.* **1969**, *24B*, 824.
(2) Araya, K. *Bull. Chem. Soc. Jpn.* **1991**, *64*, 730.
(3) Drake, A. F.; Udvarhelyi, P.; Ando, D. J.; Bloor, D.; Obhi, J. S.; Mann, S. *Polymer* **1989**, *30*, 1063.
(4) Hasegawa, T.; Ichikawa, K.; Kanetake, T.; Koda, T.; Takeda, K.; Kobayashi, H.; Kubodera, K. *Chem. Phys. Lett.* **1990**, *171*, 239.
(5) Sandman, D. J. *Mol. Cryst. Liq. Cryst.* **1990**, *189*, 273.
(6) Coyne, L. D.; Chang, C.; Hsu, S. L. *Makromol. Chem.* **1987**, *188*, 2311.
(7) Rughooputh, S. D. D. V.; Phillips, D.; Bloor, D.; Ando, D. J. *Polym. Commun.* **1984**, *25*, 242.
(8) Tokura, Y.; Ishikawa, K.; Kanetake, T.; Koda, T. *Phys. Rev. B* **1987**, *36*, 2913.
(9) Tomioka, Y.; Tanaka, N.; Imazeki, S. *J. Chem. Phys.* **1989**, *91*, 5694.
(10) Chance, R. R.; Baughman, R. H.; Müller, H.; Eckardt, C. J. *J. Chem. Phys.* **1977**, *67*, 3616.
(11) Eckhardt, H.; Boudreaux, D. S.; Chance, R. R. *J. Chem. Phys.* **1986**, *85*, 4116.
(12) Exarhos, G. J.; Risen, W. M. Jr.; Baughman, R. H. *J. Am. Chem. Soc.* **1976**, *98*, 481.
(13) Bauer, H.-D.; Materny, A.; Müller, I.; Schwoerer, M. *Mol. Cryst. Liq. Cryst.* **1991**, *200*, 205.
(14) Materny, A.; Kiefer, W. *Verhandl. DPG (VI)* **1991**, *26*, 764.
(15) Ganz, M.; Kiefer, W.; Materny, A.; Vogt, P. *J. Mol. Struct.* **1992**, *266*, 115.
(16) Materny, A.; Kiefer, W. *J. Chem. Phys.*, in press; *Phys. Rev. B*, in press; *J. Raman Spectrosc.*, in press.
(17) Lim, K. C.; Sinclair, M.; Casalnuovo, S. A.; Fincher, C. R.; Wudl, F.; Heeger, A. J. *Mol. Cryst. Liq. Cryst.* **1984**, *105*, 329.
(18) Müller, M. A.; Schmidt, M.; Wegner, G. *Makromol. Chem., Rapid Commun.* **1984**, *5*, 83.
(19) Materny, A.; Schwoerer, M.; Kiefer, W. In *Proceedings of the XIIth International Conference on Raman Spectroscopy*; Durig, J. R., Sullivan, J. F., Eds.; J. Wiley & Sons: Chichester, U.K. 1990; p 742.
(20) Materny, A.; Leuchs, M.; Michelis, T.; Schaschek, K.; Kiefer, W. *J. Raman Spectrosc.*, in press.
(21) Warta, R. Ph.D. Thesis, University of Stuttgart, 1989.
(22) Chen, Y. C.; Tripathy, S. K.; Carter, G. M.; Elman, B. S.; Koteles, E. S.; George, J., Jr. *Solid State Commun.* **1986**, *58*, 97.
(23) Sandman, D. J.; Chen, Y. J. *Polymer* **1989**, *30*, 1027.
(24) Wenzel, M.; Atkinson, G. H. *J. Am. Chem. Soc.* **1989**, *111*, 6123.
(25) Taylor, M. A.; Odell, J. A.; Batchelder, D. N.; Campbell, A. J. *Polymer* **1990**, *31*, 1116.
(26) Bloor, D.; Preston, F. H.; Ando, D. J.; Batchelder, D. N. In *Structural Studies of Macromolecules by Spectroscopic Methods*; Ivin, K. J., Ed.; J. Wiley & Sons: Chichester, U.K., 1976; p 91.
(27) Batchelder, D. N.; Bloor, D. *J. Phys. C: Solid State Phys.* **1982**, *15C*, 3005.
(28) Batchelder, D. N.; Bloor, D. J. *J. Polym. Sci., Polym. Phys. Ed.* **1979**, *17*, 569.
(29) Druet, S. A. J.; Taran, J.-P. E. *Prog. Quantum. Electron.* **1981**, 7, 1.
(30) *Non-Linear Raman Spectroscopy and Its Chemical Applications*; Kiefer, W., Long, D. A., Eds.; D. Reidel Publishing Co.: Dordrecht, The Netherlands, 1982.
(31) Gross, H.; Sixl, H. *Chem. Phys. Lett.* **1982**, *91*, 262.
(32) Schaffer, H. E.; Chance, R. R.; Silbey, R. J.; Knoll, K.; Schrock, R. R. *J. Chem. Phys.* **1991**, *94*, 4161.
(33) Brivio, G. P.; Mulazzi, E. *Phys. Rev. B* **1986**, *33B*, 2615.
(34) Eichele, H.; Schwoerer, M. *Phys. Status Solidi A* **1977**, *43*, 465.
(35) Warta, R.; Sixl, H. *J. Chem. Phys.* **1988**, *88*, 95.
(36) Pfeiffer, M.; Lau, A.; Werncke, W. *J. Raman Spectrosc.* **1990**, *21*, 835.